Available online at www.sciencedirect.com
SCIENCE DIRECT®
Physica C 408–410 (2004) 495–498
PHYSICA C
www.elsevier.com/locate/physc

# Porous vortex matter

S.S. Banerjee [a], E. Zeldov [a,*], A. Soibel [a,1], Y. Myasoedov [a], M. Rappaport [a], M. Menghini [b], Y. Fasano [b], F. de la Cruz [b], C.J. van der Beek [c], M. Konczykowski [c], T. Tamegai [d,e]

[a] Department of Condensed Matter Physics, Weizmann Institute of Science, Rehovot 76100, Israel
[b] Instituto Balseiro and Centro Atómico Bariloche, CNEA, Av. Bustillo 9500, Bariloche, RN, Argentina
[c] Laboratoire des Solides Irradiés, CNRS UMR 7642, Ecole Polytechnique, 91128 Palaiseau, France
[d] Department of Applied Physics, University of Tokyo, Hongo, Bunkyo-ku, Tokyo 113-8656, Japan
[e] CREST Japan Science and Technology Corporation (JST), Japan

**Abstract**

Structure, dynamics, and thermodynamic properties of vortex matter in the presence of a low density of columnar defects (CDs) were studied in BSCCO crystals. Magnetic decorations show that when vortices outnumber CDs a heterogeneous vortex matter is formed consisting of two populations of vortices: vortices residing on CDs form a matrix of pinned vortices, whereas the interstitial vortices form ordered crystallites within the 'pores' of the matrix. Differential magneto-optical studies reveal that at elevated fields this porous phase melts in two stages, a first-order melting of the crystallites at a temperature considerably higher than the pristine melting, and a continuous melting of the matrix at still higher temperature. At low fields the two transitions occur simultaneously, giving rise to a sharp kink in the observed melting line.


*PACS:* 74.60.Ec; 74.60.Ge; 74.80.−g; 74.72.Hs
*Keywords:* Ordered disordered vortex matter; BSCCO; Columnar defects

Vortex matter in presence of heavy-ion irradiation-induced columnar defects is generally believed to form a Bose glass (BG) phase [1] which is a strongly pinned, homogeneously disordered and anisotropic state. This description is adequate when CDs significantly outnumber vortices. In contrast, we propose here a new state of *porous* vortex matter, which occurs when vortices outnumber CDs. This *heterogeneous* phase consists of a rigid matrix created by vortices localized on the network of random CDs, and of interstitial vortices forming softer vortex nanocrystals confined within the 'pores' of the matrix. The weakly pinned nanocrystals may melt prior to the melting of the rigid matrix.

The reported findings were obtained using differential magneto-optical (MO) [2,3] and Bitter decoration [4,5] techniques. High quality $Bi_2Sr_2CaCu_2O_8$ (BSCCO) crystals ($T_c \approx 89$ K) were irradiated by 1 GeV Pb ions through various patterned masks at GANIL, with doses corresponding to matching fields of $B_\phi = 5$, 10, 20, and 50 G, where $B_\phi = n_{col}\phi_0$, $n_{col}$ is density of CDs and $\phi_0$ is the flux quantum. Fig. 1a shows schematically one of these masks, which results in the formation of CDs only within the circular apertures of about 90 μm diameter.

The analysis of the Bitter decoration in Fig. 1b [3,4] shows that in contrast to the well ordered state (Bragg glass) [6] in the unirradiated region (bottom part), the vortex state in the irradiated region (top part) is polycrystalline like. Fig. 1c shows an AFM image of etched

* Corresponding author.
*E-mail address:* eli.zeldov@weizmann.ac.il (E. Zeldov).
[1] Current address: Jet Propulsion Laboratory, California Institute of Technology, Pasadena, CA 91109, USA.

0921-4534/$ - see front matter © 2004 Elsevier B.V. All rights reserved.
doi:10.1016/j.physc.2004.03.189

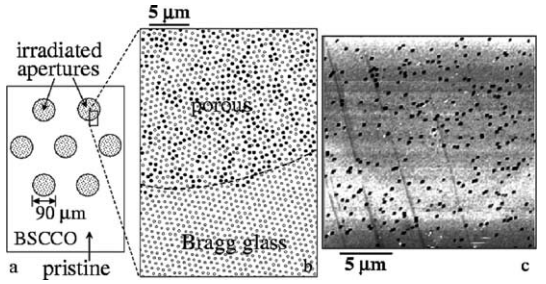


Fig. 1. (a) Schematic of BSCCO crystal irradiated through a mask with an array of circular apertures. (b) Delaunay triangulation analysis of Bitter decoration ($B = 40$ G, $T = 4.2$ K) showing pristine region at the bottom (Bragg glass) and a section of the irradiated aperture ($B_\phi = 10$ G) on top where porous vortex matter consisting of ordered crystallites embedded in a rigid matrix is formed. Open circles indicate six-fold coordinated vortices and solid dots the five and seven-fold coordinated vortices. (c) AFM image of irradiated mica etched with 40% HF revealing the location of CDs (dark spots).

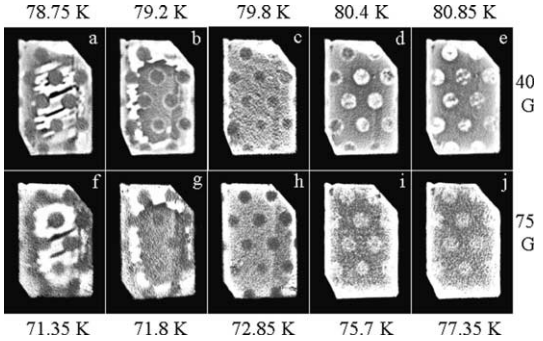


Fig. 2. Differential MO images of the melting process vs. $T$ at fields of 40 and 75 G in BSCCO crystal $0.65\times0.45\times0.01$ mm$^2$. The bright regions are the areas that undergo melting within $T$ modulation of 0.3 K. (a)–(c) and (f)–(h): melting of the pristine regions while the irradiated apertures are still solid. (d), (e) and (i), (j): melting of the irradiated apertures ($B_\phi = 20$ G). The area outside the crystal is blackened. Color MO movies are available at http://www.weizmann.ac.il/home/fnsup/.

mica that was irradiated along with the sample. Studying the distribution of CDs reveals a uniform distribution at coarse length scales. At finer scales, however, the Poisson distribution of CDs (dark spots in Fig. 1c) becomes inherently inhomogeneous with numerous sizeable voids or pores that are devoid of CDs.

Detailed analysis of the decoration data [4,5] shows that the size and distribution of vortex crystallites in Fig. 1b is consistent with the distribution of the voids. We hence conclude that when vortices outnumber CDs, there are two populations of vortices: one in which vortices that reside on CDs are strongly pinned and form a rigid matrix, and another in which the interstitial vortices are localized by significantly weaker elastic interactions and form relatively soft crystallites (open circles) trapped within the pores of the matrix. We therefore refer to this state (upper part of Fig. 1b) as 'porous' vortex matter.

Fig. 2 shows the melting process at different temperatures $T$ at two fields, 40 and 75 G. Each frame is obtained by taking the difference between the MO images at $T + 0.15$ K and $T - 0.15$ K and averaging a large number of such differential images [2]. The bright features show the regions in the sample that undergo a first-order melting transition (FOT) within the temperature interval of 0.3 K. The intensity of this bright paramagnetic signal is proportional to the equilibrium magnetization step $\Delta B$ at the transition [3,7]. Fig. 2a shows nucleation of the liquid phase (bright strip-like regions in the central part) followed by liquid expansion towards the edges (Fig. 2b), remarkably *avoiding* the irradiated apertures. In Fig. 2c the entire central pristine part of the sample is liquid, while the apertures with $B_\phi = 20$ G are still solid. In Fig. 2d the central apertures melt at 80.4 K, which is about 1.7 K above $T_m$ of the adjacent pristine regions in Fig. 2a. The $\Delta B$ step derived from the paramagnetic melting signal [7] is similar in Fig. 2d and a. Hence this is the first direct observation of an upward shift of the FOT by correlated disorder.

The melting process at 75 G (Fig. 2, second row) reveals two important differences. First, the shift of the melting temperature is more than 4 K (difference between Fig. 2i and f). Second, the $\Delta B$ in the apertures in Fig. 2i is about half of $\Delta B$ in the pristine sample. Also, the melting in each aperture is broadened over several frames, as seen by comparing Fig. 2i and j. At still higher fields, above 100 G, no paramagnetic FOT signal is detected in the irradiated apertures with $B_\phi = 20$ G.

By using differential MO with field modulation of 1 G (Fig. 3) we identify the irreversibility line at a very low effective frequency of about 0.1 Hz [2,3]. In Fig. 3a the black apertures show that the external field modulation is shielded due to the enhanced pinning, while the brighter surroundings correspond to the reversible re-

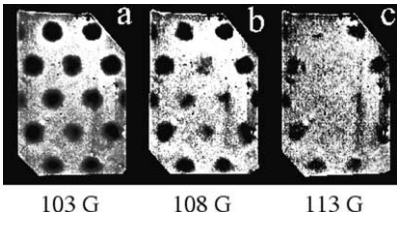


Fig. 3. Differential MO images using field modulation of 1 G in BSCCO crystal of Fig. 2 at three fields at $T = 68.4$ K. (a) All the pristine regions are liquid while the irradiated apertures ($B_\phi = 20$ G) are still solid and irreversible. (b) Partial reversibility of the central apertures. (c) Central apertures are liquid while the apertures closer to the edges begin to melt.

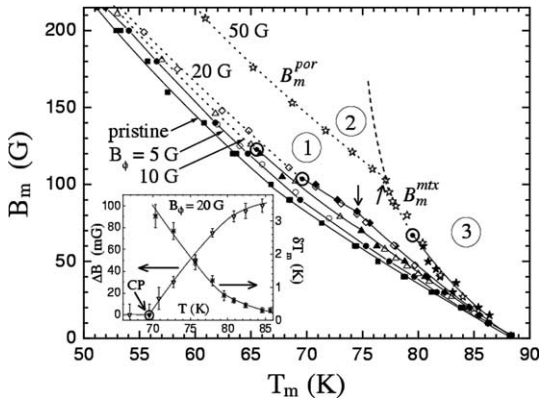


Fig. 4. The melting lines $B_m(T)$ of the pristine and irradiated regions with indicated $B_\phi$. Solid (open) symbols are temperature (field) modulation data showing the location of the FOT (irreversibility line). Solid (dotted) lines are guides to the eye of the first-order (continuous) transitions that terminate at the critical points (⊙). Inset: The height of the FOT equilibrium magnetization step $\Delta B$ that vanishes at the CP, and the local width $\delta T_m$ of the FOT vs. $T$.

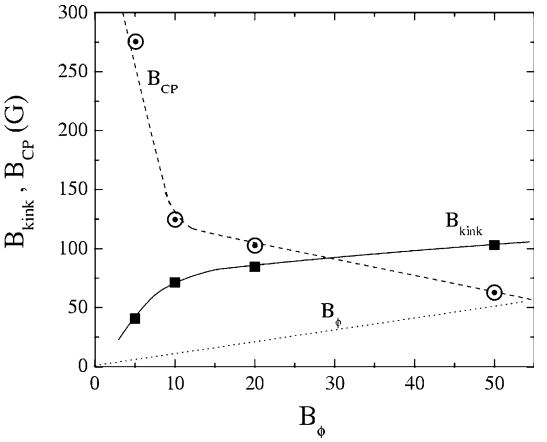


Fig. 5. The fields of the kink, $B_{kink}$ (marked by arrows in Fig. 4) and of the CP, $B_{CP}$ (marked by ⊙ in Fig. 4) versus $B_\phi$. The dotted line represents the $B = B_\phi$ line.

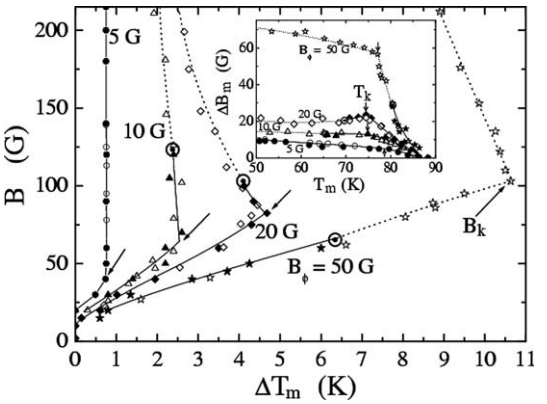


Fig. 6. The shift $\Delta T_m$ in the melting temperature for different $B_\phi$ with respect to the pristine $T_m$ at various fields $B$. Inset: The upward shift $\Delta B_m$ in the melting field vs. $T_m$.

sponse of the liquid in the pristine regions. Upon increasing the field the black apertures disappear (Fig. 3b and c) revealing the value of the local irreversibility field.

Fig. 4 shows the location of the onset of the FOT (solid symbols) for $B_\phi = 0$ (pristine), 5, 10, 20, and 50 G and of the irreversibility line (open symbols). The solid lines through the FOT data points terminate at novel critical points (CP). The CP is the point at which $\Delta B$ vanishes and the width of the melting ($\delta T_m$) becomes very broad (see inset of Fig. 4). The irreversibility data coincide with the FOT line below the CP and smoothly extrapolate the location of the transition line to higher fields. The field of the CP, $B_{CP}$, decreases with $B_\phi$ as shown in Fig. 5.

Interestingly, although the structures of the porous vortex matter and of the Bragg glass are very different (Fig. 1b), the phase diagrams for $B_\phi = 0$ and 5 G in Fig. 4 are almost identical, with a slight upward shift of the FOT. This brings us to an important conclusion that the quasi-long-range order that characterizes the Bragg glass (bottom portion of Fig. 1b) is not an essential requirement for the existence of a FOT [4,8]. The upward shift of the FOT line can be argued to arise from enhanced confinement of the soft crystallites within the rigid walls of the matrix. The confinement suppresses the effect of thermal fluctuations of the vortices thereby enhancing their melting temperature.

We now discuss another key finding which is a kink in the $B_m(T)$ lines marked by the arrows in Fig. 4. A plot of the temperature shift $\Delta T_m$ between the irradiated and pristine melting lines in Fig. 6, reveals the kink location prominently. Unlike the kink in BG theory [1,9], here the effect of CDs is more pronounced at fields above the kink, where the shift in field $\Delta B_m$ between the $B_m(T)$ of the pristine and irradiated regions (see Fig. 6 inset) is almost constant ($\approx B_\phi$), and it collapses rapidly at $T > T_k$. This collapse occurs at $T_k \sim 75$ K, with little dependence on $B_\phi$.

The observed findings can be explained by intersection of two separate melting lines, viz., $B_m^{por}$ and $B_m^{mtx}$ lines in Fig. 4. In region 1 (with respect to $B_\phi = 50$ G curve in Fig. 4) the crystallites in the pores are stabilized by the rigid matrix and remain solid up to $B_m^{por}$, well above the pristine melting line. We propose that region 2 is an interstitial liquid phase [10] in which vortices pinned on CDs coexist with surrounding liquid vortices for $B > B_{kink}$. The $B_m^{mtx}$ line describes melting or delocalization of the pinned matrix, resulting in a homogeneous liquid in region 3. This unconventional crossing of $B_m^{por}$

and $B_m^{mtx}$ lines results in the sharp kink in $B_m(T)$. At $B < B_{kink}$ the crystallites remain solid up to the collapse of the matrix. Fig. 5 shows that $B_{kink} \gg B_\phi$ in contrast to theoretical expectations [10]. Note that $B_{kink}$ and $B_{CP}$ have opposite dependence on $B_\phi$ as shown in Fig. 5, and thus at low doses the kink occurs along FOT while at higher doses along the continuous transition.

In summary, when vortices outnumber CDs the heterogeneity of the vortex system is a key element that governs the properties of the 'porous' vortex matter. At $B > B_{kink} > B_\phi$, interstitial vortex crystallites melt separately from the melting of the pinned matrix, while at $B < B_{kink}$ a single melting transition is found.

## Acknowledgements

This work was supported by the Israel Science Foundation—Center of Excellence Program, by the German-Israeli Foundation GIF, by the Minerva Foundation, Germany, and by the Grant-in-Aid for Scientific Research from the Ministry of Education, Culture, Sports, Science and Technology, Japan. EZ and FC acknowledge the support by the Fundacion Antorchas—WIS collaboration program and by the US–Israel Binational Science Foundation (BSF).

## References

[1] G. Blatter et al., Rev. Mod. Phys. 66 (1994) 1125;
D.R. Nelson, V.M. Vinokur, Phys. Rev. Lett. 68 (1992) 2398;
A.I. Larkin, V.M. Vinokur, Phys. Rev. Lett. 75 (1995) 4666.
[2] A. Soibel et al., Nature 406 (2000) 282;
A. Soibel et al., Phys. Rev. Lett. 87 (2001) 167001;
M. Yasugaki et al., Phys. Rev. B 65 (2002) 212502.
[3] S.S. Banerjee et al., Phys. Rev. Lett. 90 (2003) 087004.
[4] M. Menghini et al., Phys. Rev. Lett. 90 (2003) 147001.
[5] H. Dai et al., Science 265 (1994) 1552.
[6] T. Giamarchi, P. Le Doussal, Phys. Rev. Lett. 72 (1994) 1530.
[7] N. Morozov et al., Phys. Rev. B 54 (1996) R3784.
[8] S. Colson et al., Phys. Rev. Lett. 90 (2003) 137002.
[9] C.J. van der Beek et al., Phys. Rev. Lett. 86 (2001) 5136;
L. Krusin-Elbaum et al., Phys. Rev. Lett. 72 (1994) 1914.
[10] L. Radzihovsky, Phys. Rev. Lett. 74 (1995) 4923;
P. Sen, N. Trivedi, D.M. Ceperley, Phys. Rev. Lett. 86 (2001) 4092;
Y. Nonomura, X. Hu, <cond-mat/0212609>.